Drug Design, Development and Therapy

Dovepress
open access to scientific and medical research

Open Access Full Text Article

ORIGINAL RESEARCH

Effects of Qi Teng Xiao Zhuo granules on circRNA expression profiles in rats with chronic glomerulonephritis

This article was published in the following Dove Press journal:
Drug Design, Development and Therapy

Jia-Rong Gao[1]
Nan-Nan Jiang[2]
Hui Jiang[1]
Liang-Bing Wei[1]
Ya-Chen Gao[3]
Xiu-Juan Qin[1]
Meng-Qing Zhu[2]
Jing Wang[2]

[1]Department of Pharmacy, The First Affiliated Hospital of Anhui University of Chinese Medicine, Hefei, People's Republic of China; [2]College of Pharmacy, Anhui University of Chinese Medicine, Hefei, People's Republic of China; [3]Department of Nephrology, The First Affiliated Hospital of Anhui University of Chinese Medicine, Hefei, People's Republic of China

Objectives: To screen and study circular RNA (circRNA) expression profiles in QTXZG-mediated treatment of chronic glomerulonephritis (CGN) induced by adriamycin in rats and to research the possible roles and molecular mechanisms of QTXZG.

Materials and methods: Next-generation RNA sequencing was used to identify circRNA expression profiles in CGN after QTXZG treatment compared with a CGN model group and a control group. Bioinformatics analysis was performed to predict potential target miRNAs and mRNAs. GO and pathway analyses for potential target mRNAs were used to explore the potential roles of differentially expressed (DE) circRNAs.

Results: We identified 31 and 21 significantly DE circRNAs between the model group vs the control group and the model group vs the QTXZG group, respectively. Four circRNAs that resulted from the establishment of the CGN model were reversed following treatment with QTXZG. Further analysis revealed that these four circRNAs may play important roles in the development of CGN.

Conclusions: This study elucidated the comprehensive expression profile of circRNAs in CGN rats after QTXZG treatment for the first time. Analysis of the circRNA–miRNA–mRNA–ceRNA network to determine potential function provided a comprehensive understanding of circRNAs that may be involved in the development of CGN. The current study indicated that therapeutic effects of QTXZG on CGN may be due to regulation of circRNA expression.

Keywords: CGN, Qi Teng Xiao Zhuo granules, circRNA, next-generation sequencing

Introduction

Chronic glomerulonephritis (CGN) is the major component of chronic kidney disease (CKD), and the most common cause of end-stage kidney disease, CGN. CGN causes significant pain and imposes societal and economic burdens on national health systems. Moreover, CGN incidence is continuously growing, resulting in increased mortality.[1] The immune-mediated inflammatory response in the tubulointerstitial compartment and glomerular damage play a key role in the progression of CGN.[2] CGN patients suffer from many severe clinical symptoms and reduced renal function.[3,4]

Western medicines used to treat CGN include corticosteroids, immunosuppressors, angiotensin-converting enzyme inhibitors, angiotensin II receptor blockers, and cyclophosphamide.[5] Efficacy of these drugs is insufficient and costs are very high. Furthermore, these drugs are associated with serious side effects when administered long term.[3,6]

Correspondence: Jia-Rong Gao
Department of Pharmacy, The First Affiliated Hospital of Anhui University of Chinese Medicine, 117 Meishan Road, Hefei 230031, People's Republic of China
Tel +865 516 283 8553
Fax +865 516 283 8553
Email zyfygjr2006@163.com

submit your manuscript | www.dovepress.com
DovePress
http://doi.org/10.2147/DDDT.S191386

In traditional Chinese medicine (TCM), CGN belongs to the diagnostic criteria: "spleen deficiency, blood stasis, and damp". Xin'an medicine, an important academic school of TCM, which originated in the Song dynasty (960-1279AD), states that "spleen deficiency, damp, and blood stasis" play key roles in CGN. Based on this theory, a famous elder TCM doctor of Xin'an medicine presented "invigorating the spleen and water, removing blood stasis" to treat CGN.[7–9] QTXZG (approval number: Anhui province Food and Drug Administration, Z20070001) was developed based on this theory. QTXZG, also known as Shenkang granula or infusion, consists of the following herbal medicines: Astragalus membranaceus (Fisch.) Bunge. (Astragali Radix, Milkvetch Root, Huangqi); Coix lacryma-jobi L. (Coicis Semen, Jobstears Seed, Yiyiren); Tripterygium wilfordii Hook. f. (Tripterygium wilfordii, Leigongteng); Cryptotympana pustulata Fabricius (Cicdae Periostracum, Cicada Slough, Chantui); Hedyotis diffusa Willd. (Spreading Hedyotis Herb, Baihuasheshecao); Imperata cylindrica Beauv . var. major (Nees) C. E. Hubb. (Imperatae Rhizoma, Cogongrass Rhizome, Baimaogen); Leonurus japonicus Houtt. (Leonuri Herba, Wormwoodlike Motherwort, Yimucao). The functions of these herbal medicines as annotated in Chinese Pharmacopoeia 2015 include: tonifying spleen, inducing diuresis to reduce edema, promoting blood circulation to remove blood stasis, clearing heat, and detoxifying, which corresponding to TCM theory of pathogenesis of CGN. These herbal medicines have been widely applied to treat CGN at home and abroad.[10–12]

QTXZG has been used for clinical treatment of CGN for more than 20 years. It was shown to be effective in relieving clinical symptoms with no obvious toxic side effects.[13,14] The mechanisms of action of QTXZG may be regulation of immune function, reduction of urine protein, inhibition of the inflammatory response, and improvement of coagulation.[15–17] Our previous study showed that QTXZG was effective for treatment of CGN in an adriamycin-induced CGN rat model. Mechanisms involved in these effects included regulation of expression of inflammatory factors, regulation of inflammatory gene expression profiles, and inhibition of the Syk/Ras/c-Fos signaling pathway.[3,18,19] However, the specific and comprehensive mechanisms of action have not been characterized.

Our previous study demonstrated appropriate methods for the extraction and preparation of QTXZG.[20] Our previous quality control study demonstrated that we could identify Astragalus Membranaceus and Hedyotis diffusa Willd, and perform a limit for Wilforlide A using thin layer chromatography (TLC). In addition, Astragaloside iv content could be measured using thin layer scanning (TLS).[21] Moreover, we performed another study aimed at improving quality standards in which we showed that we could identify Hedyotis diffusa Willd, Leonurus japonicus Houtt, Coix lacryma-jobi L, and Cryptotympana pustulata Fabricius by TLC. In addition, we were able to determine calycosin-7-glucoside content, of a component of Astragalus Membranaceus, by high-performance liquid chromatography.[22] The methods used for control quality were simple, specific, accurate, and reliable.

Recent advances in sequencing and bioinformatics technology have indicated that protein-coding and noncoding genes are not only expressed as linear messenger RNAs but as covalently closed circular RNAs (circRNAs).[23] CircRNAs are stable, abundant, and conserved and could regulate gene expression in eukaryotes.[24] Moreover, numerous studies have used miRNA sponging, which regulates transcription of miRNA-target genes, to demonstrate that specific circRNAs are involved in various diseases, including kidney diseases.[25–28] However, circRNA dysregulation in CGN after QTXZG treatment has not been studied.

In our study, we evaluated the circRNAs expression profile of in adriamycin-induced CGN rats following QTXZG treatment, and predicted potential functions of these circRNAs. We believe that our findings will advance understanding of the possible mechanism of QTXZG in treatment for CGN and may identify novel circRNAs as potential therapeutic targets.

Materials and methods

Chemicals

Adriamycin was purchased from Pfizer Pharmaceuticals Ltd. (Wuxi, People'sRepublic of China), batch number: N97872. QTXZG was obtained from the First Affiliated Hospital of Anhui University of Chinese Medicine (Hefei, People's Republic of China), batch number: 20171106. Chloral hydrate was obtained from Shanghai chemical reagent company (Shanghai, People's Republic of China).

Animal model[3]

All experiments were subject to approval by the Experiments Animal Ethics Committee of Anhui University of Chinese Medicine, Hefei, China. Number of animals and pain were reduced as much as possible. All experiments were in accordance with the "Implementation Rules for the Management of Medical Laboratory Animals" issued by the Ministry of Health of the People's Republic of China and the "Regulations for the Administration of Affairs

Concerning Experimental Animals" issued by the National Science and Technology Commission. All surgeries were performed under chloral hydrate anesthesia.

Thirty male Sprague-Dawley rats (250±20 g, 8 weeks old, . grade) were obtained from Jiesijie experimental animal co. ltd (Shanghai, People's Republic of China). All animals were healthy and had never taken any medication. Animals were held in a controlled room with the temperature set to 18–22°C and humidity set to 40–60%. The animals were allowed food and water ad libitum.

The animals were allowed to acclimate for 1 week, then were randomly assigned to three groups: control group, model group, and QTXZG group, 10 rats in each group. Each rat in the model and QTXZG groups was injected with adriamycin through the tail vein twice: 4.0 mg/kg on the 1st day and 3.5 mg/kg on the 14th day. On the 21st day, all rats were placed in metabolic cages to collect urine for 24 hrs. 24 -hr urine protein content was tested. A successful model was indicated by 24 -hr urinary protein content >50 mg/kg.

After the CGN model was established successfully, each rat in the QTXZG group was given QTXZG (10.8 g/kg) by gavage once per day for 30 days. Simultaneously, solvent (10.8 g/kg) was administered to rats in the control and model groups.

After the last administration of medication, nine rats were randomly selected from the three groups, three rats from each group. Rats were anesthetized using 3.5% chloral hydrate solution (1 mL/kg, IP). Kidneys were quickly excised, the rats were sacrificed, and glomerular samples were collected. Each specimen was packaged individually and stored at −80°C for further analysis.

Histological observation

Glomerular samples were collected and fixed in 10% neutral formalin. Histological alterations were observed by H&E staining.

Identified DE circRNAs[29]

RNA isolation and quality control

Following the manufacturer´s instructions, total RNA was extracted using miRNeasy Mini Kit (Cat#217004, Qiagen). A NanoDrop ND-2000 spectrophotometer (Thermo Fisher Scientific, Waltham, MA, USA) was used to quantify RNA concentration. RNA integrity was assessed using an Agilent Bioanalyzer 2100 (Agilent technologies, Santa Clara, CA, USA). RNA was purified using RNA Clean XP Kit (Cat#A63987, Beckman Coulter, Inc. Kraemer Boulevard Brea, CA, USA) and RNase-Free DNase Set (Cat#79254, Qiagen, GmbH, Germany).

cDNA library construction and quality control

Following the manufacturer's instructions, ribosomal RNA (rRNA) was depleted. Then, ethanol precipitation was used to clean the rRNA-free material. Ribosomal-depleted RNA was fragmented and reverse transcription was performed using a random primer to produce first strand cDNA. Second strand cDNA was synthesized using DNA polymerase Ⅰ and RNase H digestion, dUPTs was mixed in to replace dTTPs in the reaction buffer. Next, end-repair/dA-Tailing and adapter ligation were performed. The ligated-product was purified to select cDNA fragments sized 150–200 bp. PCR amplification of cDNA libraries was carried out for 15 cycles. The amplified product was cleaned using VATHTS DNA Clean Beads. After the post-amplification purification procedure, cDNA libraries were stored at −20°C. Quality control of the cDNA libraries and quantification of cDNA were performed using an Agilent Bioanalyzer 2100. Origin biotech Inc (Shanghai, People'sRepublic of China) performed next-generation RNA sequencing.

Data analysis

RNA-sequenced raw reads in FASTQ format were filtered with Seqtk software (http://github.com/lh3/seqtk). Filtering processes included: removing the reads containing adapter sequences, wiping off low-quality reads and the rRNA reads of rats. BWA-MEM alignment algorithm was used to align the clean reads to the reference genome.[30] CIRI software was applied to predict circRNAs.[31] We classified the predicted circRNAs via perl scripts. By calculating the expression of the back-splicing junction reads, we identified expression of circRNAs. SPRBM was used to normalize the reads. EdgeR was used to identify DE circRNAs.[32] CircRNAs exhibiting P-values <0.05 with log2-fold change >2 were identified as significant.

Bioinformatics analysis

Based on miRanda (http://www.microrna), we predicted potential miRNA targets for significantly dysregulated circRNAs via Origin biotech home-made miRNA target prediction software.[33] The putative mRNA targets of the miRNAs mentioned above were predicted by mirWalk and mircoT-CDS. Cytoscape (http://cytoscape.github.io/) was used to delineate the circRNA–miRNA–mRNA ceRNA network.[34]

Clusterprofiler software was used to analyze biological functions of potential target mRNAs using gene ontology (GO) analysis. GO analysis was evaluated for three aspects: biological processes (BP), molecular functions (MF), and cellular components. We also analyze the related pathways via KEGG.

qRT-PCR validation

Four significantly dysregulated circRNAs were measured by quantitative real-time PCR. Following the manufacturer´s instructions, total RNA was extracted using miRNeasy Mini Kit (Cat#217004, Qiagen). The concentration and purity of RNA were determined using a NanoDrop ND-2000 spectrophotometer (Thermo Fisher Scientific, Waltham, MA, USA). Total RNA was reverse-transcribed into cDNA using RevertAid First Strand cDNA Synthesis Kit (Thermo Fisher Scientific, Waltham, MA, USA). Using specific primers (Table 1), qRT-PCR reactions were performed using FastStart Universal SYBR Green Master (Rox). Reactions proceeded using the following conditions: 95°C for 10 mins followed by 40 cycles of 95°C for 15 s, 60°C for 60 s. Melting curves ranging from 60°C to 95°C were included in each run.

Statistical analysis

SPSS 23.0 (IBM Corporation, Armonk, NY, USA), software was used for data analysis. Quantitative data were expressed as mean±SD. Student's *t*- test was used to determine the difference between two groups, and one-way ANOVA was used to assess differences among multiple groups. Differences with $P<0.05$ were considered statistically significant.

Results

Histopathology

As shown in Figure 1, the model group showed the following characteristics compared to the control group: the renal interstitium were congestive, oedematous, and infiltrated by inflammatory cells, the convoluted tubules were curved and expanded, protein casts were evident in renal tubular lumen, and glomerular basement membrane thickness (GBMT) was increased. The QTXZG group showed less inflammatory cells and protein casts, and thickness of the GBMT was reduced compared to control.

Table 1 Data process

Samples ID	Raw reads	Clean reads	Clean ratio	rRNA trimmed	rRNA ratio	No rRNA pair	Mapped reads	Mapping ratio (%)
Control-1	81,268,140	77,969,803	95.94%	77,831,844	0.18%	75,956,310	75,685,335	99.64
Control-2	76,908,614	73,639,495	95.75%	73,542,223	0.13%	71,618,418	70,954,789	99.07
Control-3	89,439,130	85,488,819	95.58%	85,397,535	0.11%	82,809,618	82,597,749	99.74
Model-1	73,507,996	68,959,127	93.81%	68,818,843	0.20%	65,683,196	65,197,092	99.26
Model-2	73,599,894	70,837,843	96.25%	70,648,310	0.27%	69,050,466	68,537,309	99.26
Model-3	72,480,624	69,769,335	96.26%	69,425,424	0.49%	67,703,444	67,663,323	99.94
QTXZG-1	79,270,590	76,412,082	96.39%	76,272,159	0.18%	74,794,546	74,760,919	99.96
QTXZG-2	89,580,760	86,210,744	96.24%	86,096,190	0.13%	83,985,080	83,936,219	99.94
QTXZG-3	66,928,610	63,425,128	94.77%	63,336,307	0.14%	60,821,570	60,323,265	99.18

Notes: Clean ratio=(clean reads/raw reads) %; rRNA ratio= [(clean reads – rRNA trimmed)/clean reads] %.

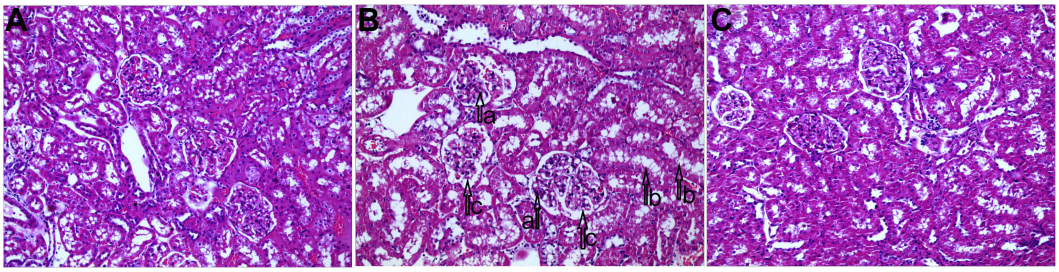

Figure 1 Histological alterations(magnification, ×200). (**A**) control group; (**B**) model group; (**C**) QTXZG group. (**a**) Inflammatory cells; (**b**) protein casts; (**c**) thickened GBMT.
Abbreviation: glomerular basement membrane thickness.

Table 2 Part of the interactions between miRNAs and circRNAs

miRNA ID	Max energy	Query_seq(3′-5′)	Ref_seq(5′-3′)
circRNA-213			
miR-346	−21.2	ucuccgUCCGUGAGUCCGUCUGu	aagctgAGGTGAT–GGCAGACa
circRNA-89			
miR-342-3p	−20.59	ugcccacGCUAAAGACACACUCu	ggagtctTGATT–TGTGTGAGg
circRNA-3217			
miR-326-3p	−21.36	ugaccUCCUUCCC—GGGUCUCc	cggatAGCTAGGGTTACCCAGAGa
circRNA-4907			
miR-149-5p	−28.25	cccucACUUCUGUG-CCUCGGUCu	cagtcTGGGGACACATGAGCCAGa
miR-125b-5p	−24.59	agUGUUCAAUCCCAGAGUCCCu, aguguucaAUCCC—AGAGUCCCu, agugUUCAAUCCCAGAGUCCCu	gtGTGAGGTGGAATCTCAGGGt, ttctgcacTAGGGTCATCTCAGGGc, atggAAGTT–GTACTCAGGGa

Note: Max energy: the energy of the dimer formed by miRNA and circRNA where the smaller the max energy, the closer the combination between circRNAs and miRNAs.

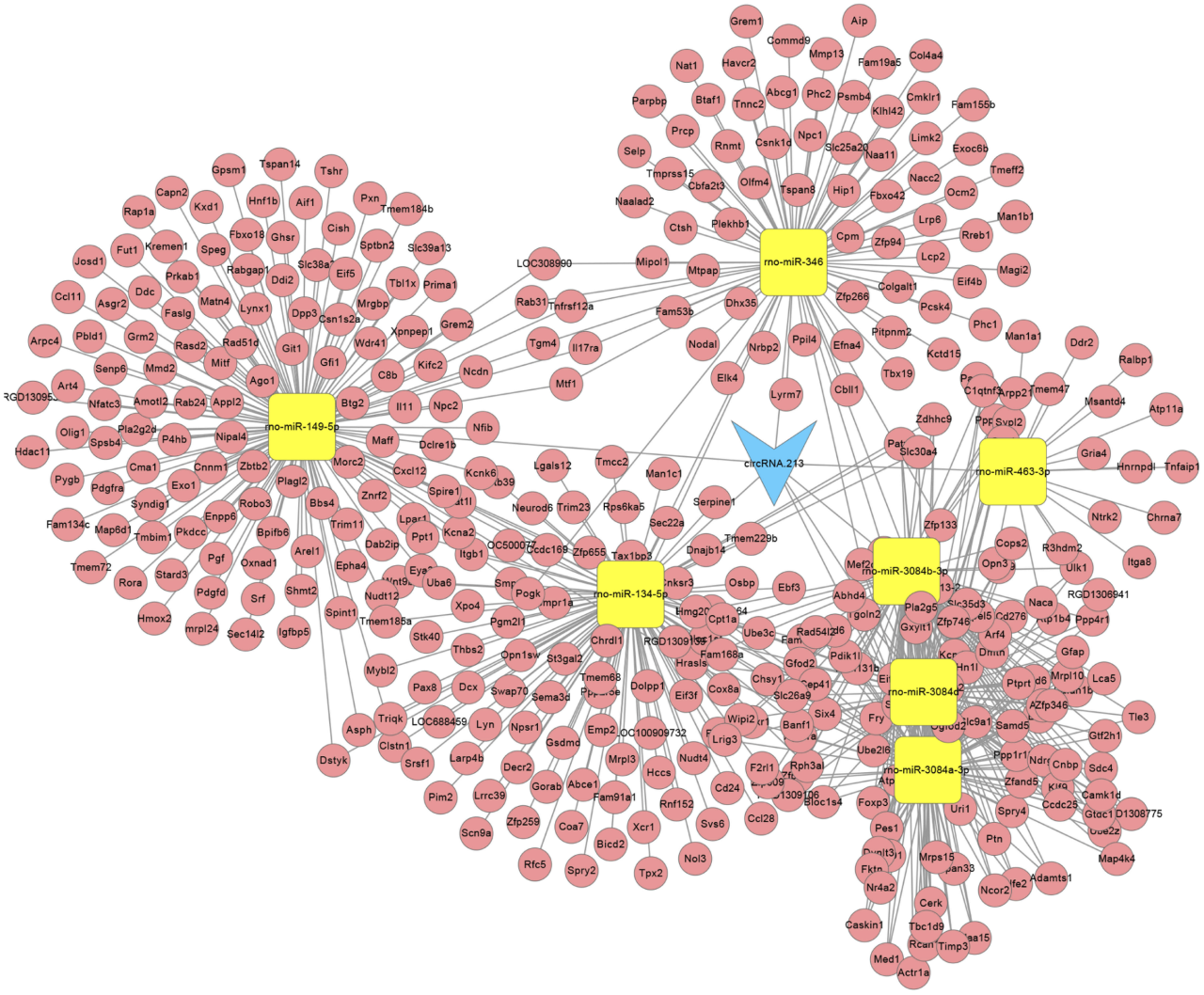

Figure 2 The subnetwork of circRNA-213. A total of 7 miRNA nodes, 392 mRNA nodes, and 629 edges were included. CircRNA-213 is represented by a blue arrow, and miRNAs and mRNAs are represented by yellow squares and pink circles, respectively.

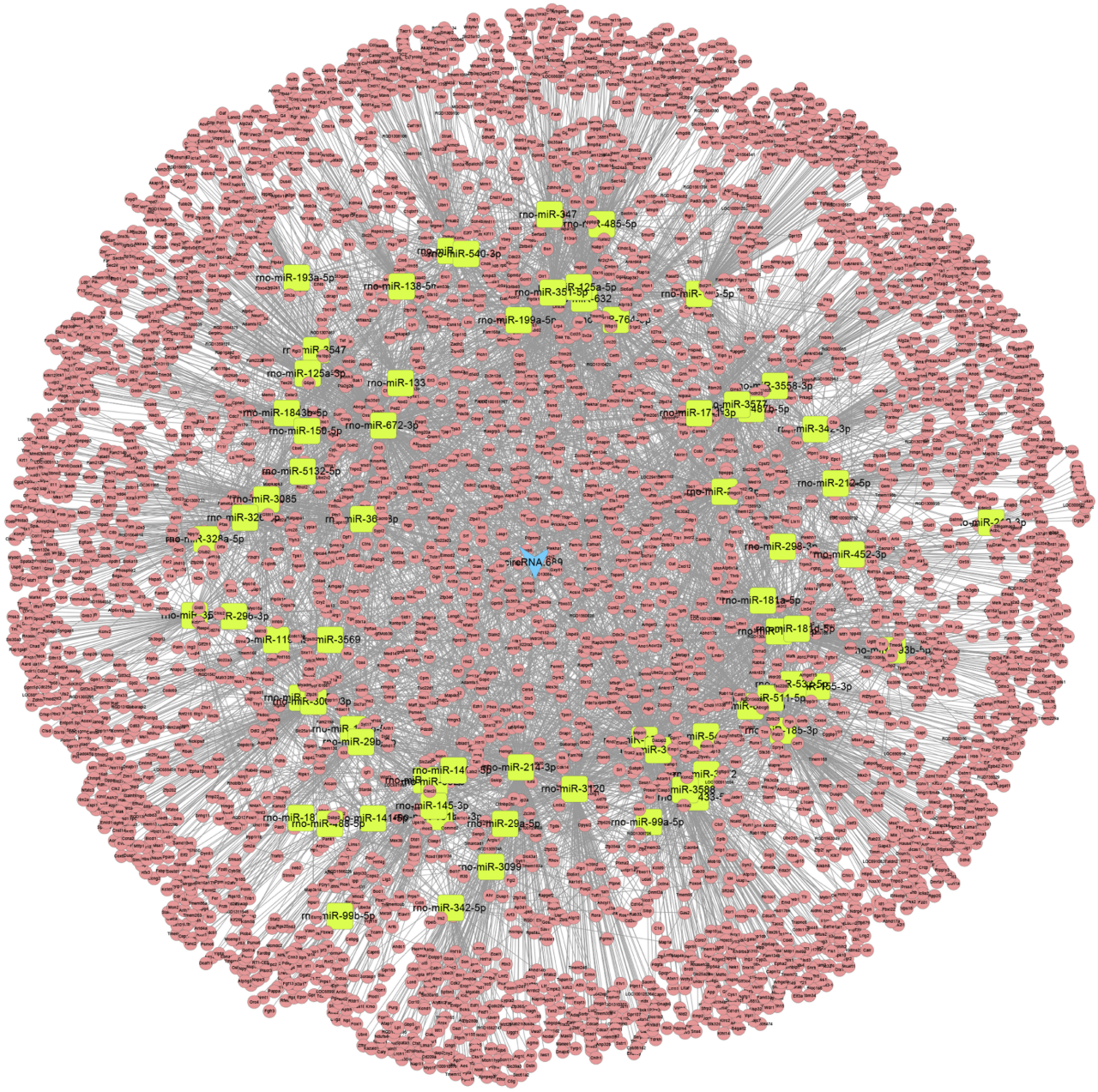

Figure 3 The subnetwork of circRNA-689. A total of 71 miRNA nodes, 37,88 mRNA nodes, and 7,134 edges were included. CircRNA-689 is represented by a blue arrow, and miRNAs and mRNAs are represented by yellow squares and pink circles, respectively.

Identifying the DE circRNAs

After NGS, filtration and quality control were conducted to obtain clean reads. Clean reads were abundantly expressed. Next, rRNA was trimmed, and more than 99% of the no rRNA pair reads were mapped to the genome in the glomerular tissues. The data process is displayed in Table 1.

After the integration of the data, 5,363 circRNAs were identified from the nine samples (Supplementary material). We set the following screening criteria: FC>2 and *P*-value <0.05. There were 31 significantly DE circRNAs between the model group and the control group, and 21 significantly DE circRNAs between the model group and the QTXZG group. DE circRNAs were further analyzed, and four circRNAs (circRNA-213, 689, 3217 and 4907) altered due to the establishment of the CGN model establishing were reversed via the treatment of QTXZG.

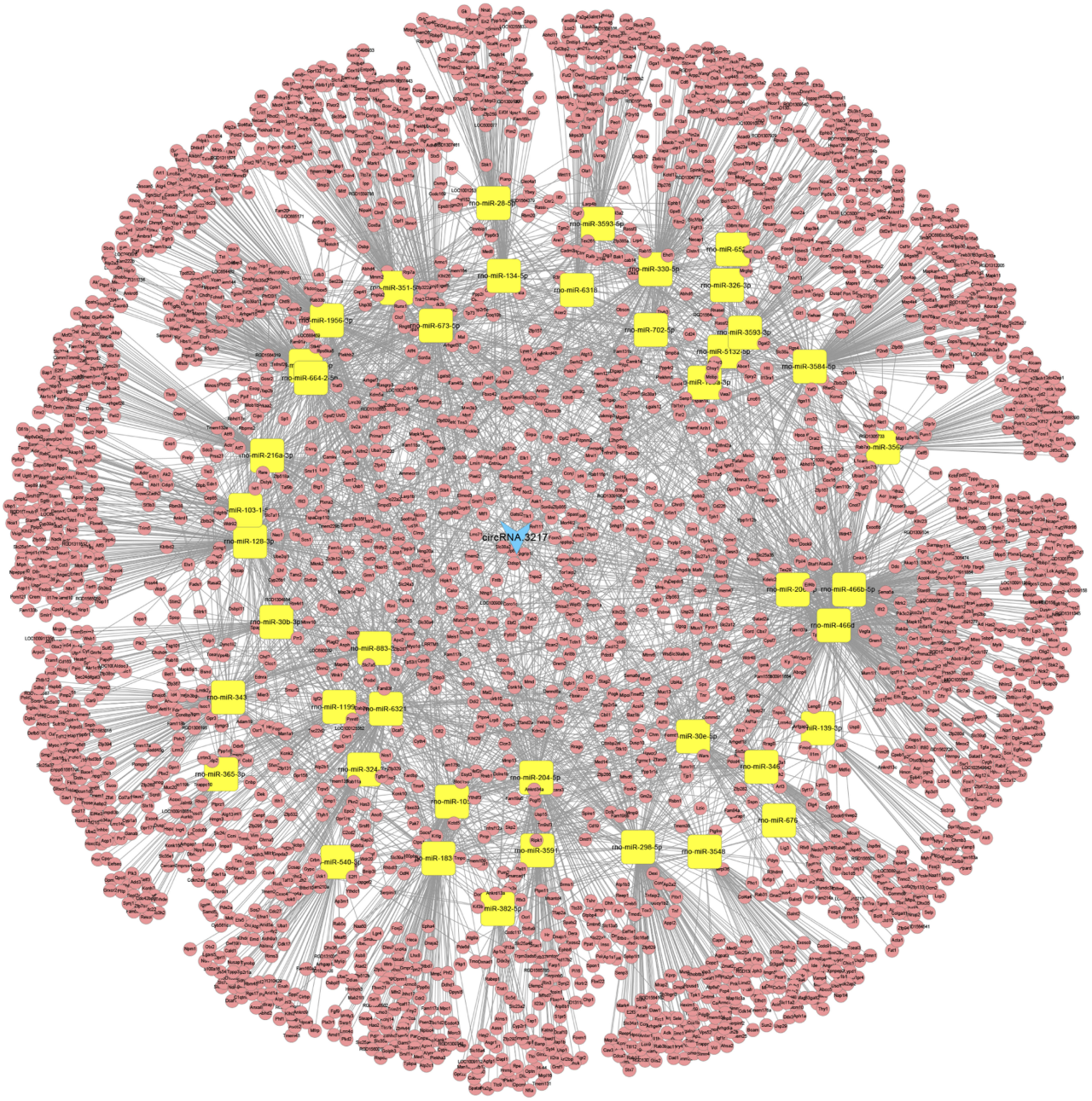

Figure 4 The subnetwork of circRNA-3217. A total of 44 miRNA nodes, 2973 mRNA nodes, and 4,909 edges were included. CircRNA-3217 is represented by a blue arrow, and miRNAs and mRNAs are represented by yellow squares and pink circles, respectively.

Bioinformatics analysis

Prediction of circRNA–miRNA interactions

CircRNAs could participate in multiple diseases via sponging miRNAs.[25] We predicted the potential target miRNAs of four circRNAs based on conserved seed-matching sequence. The results showed that all of four circRNAs contained at least seven respective miRNA response elements. Interactions between miRNAs and circRNAs are listed in Table 2.

Prediction of circRNA-miRNA-mRNA ceRNA network for each circRNA

Putative target genes were predicted and circRNA–miRNA–mRNA ceRNA networks were delineated. The CircRNA-213–miRNA–mRNA network (Figure 2) included 7 miRNA nodes, 392 mRNA nodes, and 629 edges. Figure 3 shows the ceRNA network of circRNA-689, which contained a total of 71 miRNA nodes, 3,788 mRNA nodes, and 7,134 edges. For circRNA-3217, the subnetwork included 44 miRNA nodes,

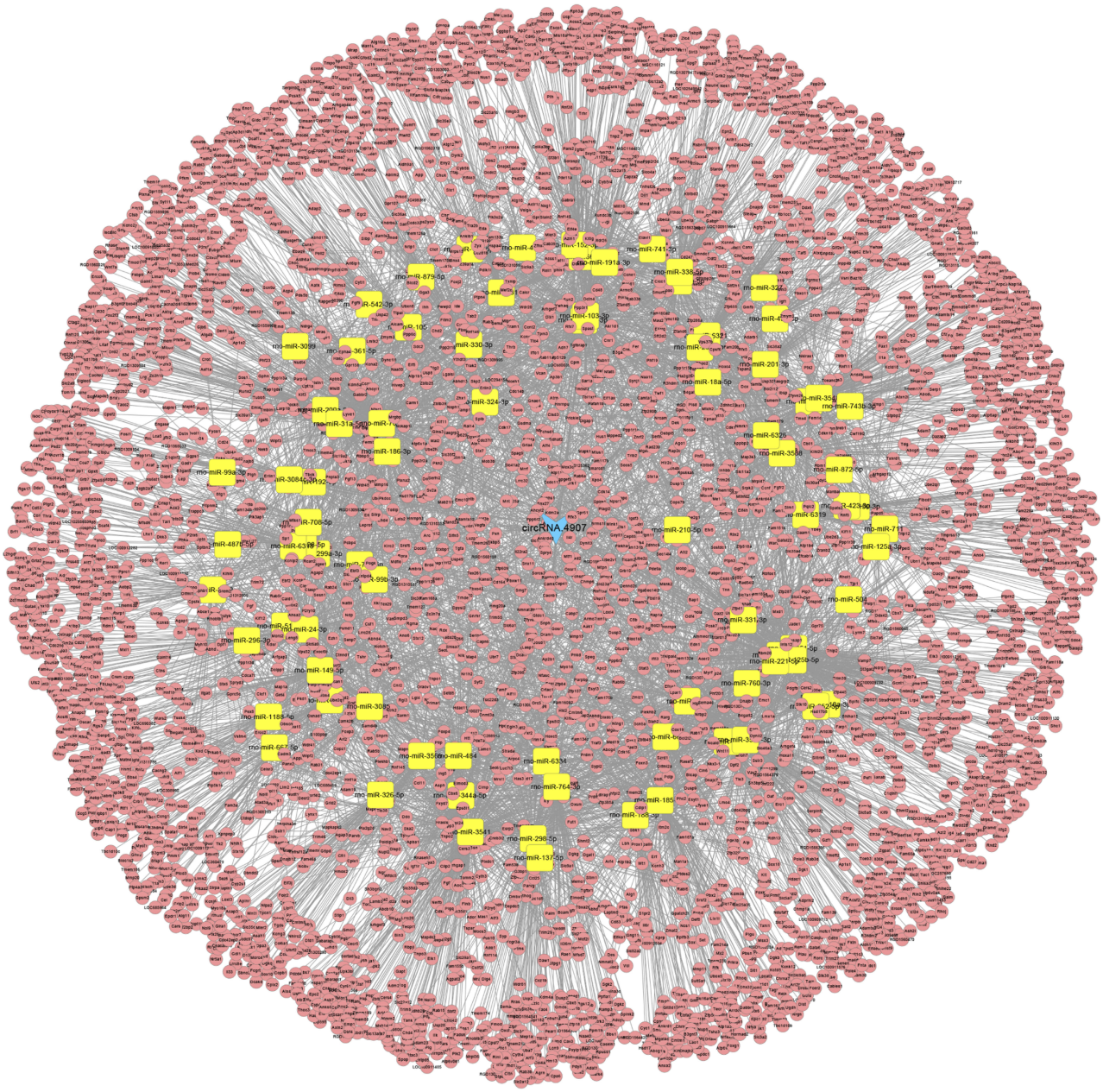

Figure 5 The subnetwork of circRNA-4907. A total of 84 miRNA nodes, 3,985 mRNA nodes, and 7,946 edges were included. CircRNA-4907 is represented by a blue arrow, and miRNAs and mRNAs are represented by yellow squares and pink circles, respectively.

2,973 mRNA nodes, and 4,909 edges (Figure 4). In the circRNA-4907–miRNA–mRNA network (Figure 5), there were 84 miRNA nodes, 3,985 mRNA nodes, and 7,946 edges. In each subnetwork, blue arrows represent circRNA, yellow squares represent miRNAs, and pink circles represent mRNAs.

Potential biological functions and pathways

To further explore the potential functions of circRNAs, GO, and KEGG pathways were analyzed using all putative target genes of miRNAs. 1,543 GO terms and 135 pathways were enriched in the network of circRNA.213; 5,074 GO terms and 218 pathways were enriched in the network of circRNA-689; 4,526 GO terms and 214 pathways were enriched in the network of circRNA-3217; 5,235 GO terms and 220 pathways were enriched in the network of circRNA-4907. The top 30 enrichments are shown in Figures 6–9.

Most genes were enriched in the BP terms regulation of cell differentiation, cell migration and monocyte chemotaxis, negative regulation of VEGF receptor and protein

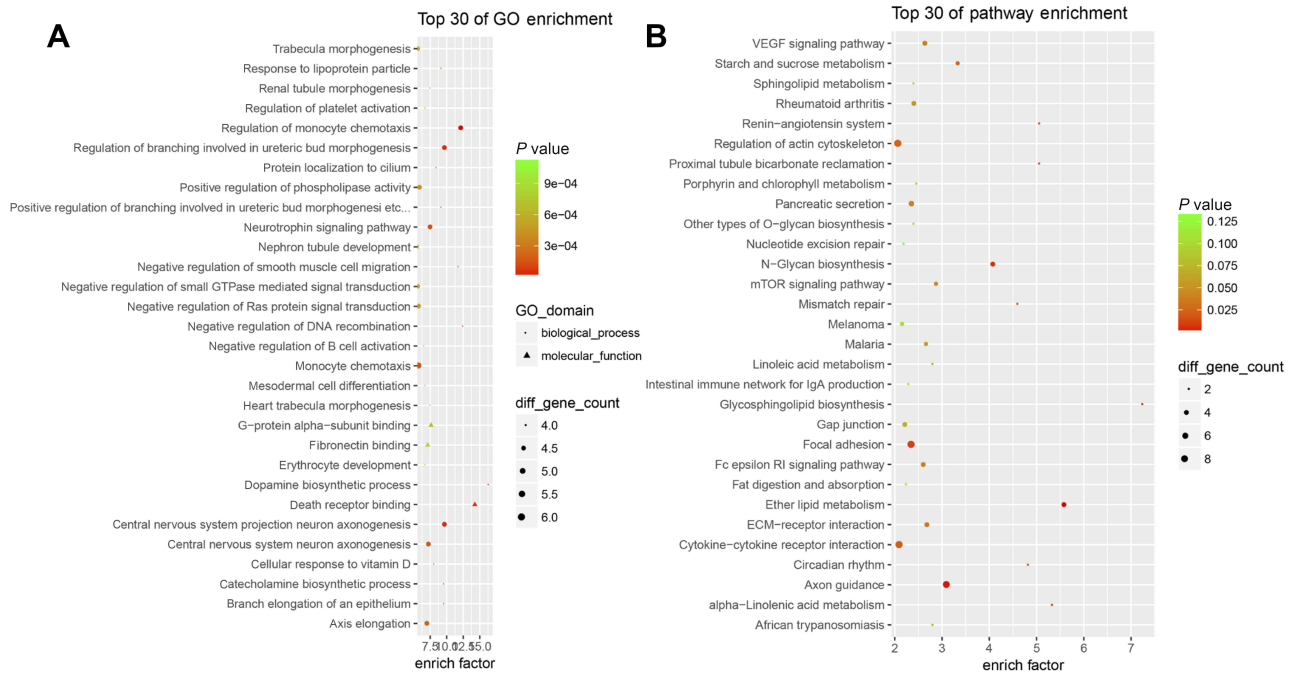

Figure 6 GO and KEGG analyses of potential target genes of circRNA-213. (**A**) Top 30 enrichment GOs. (**B**) Top 30 enrichment pathways.

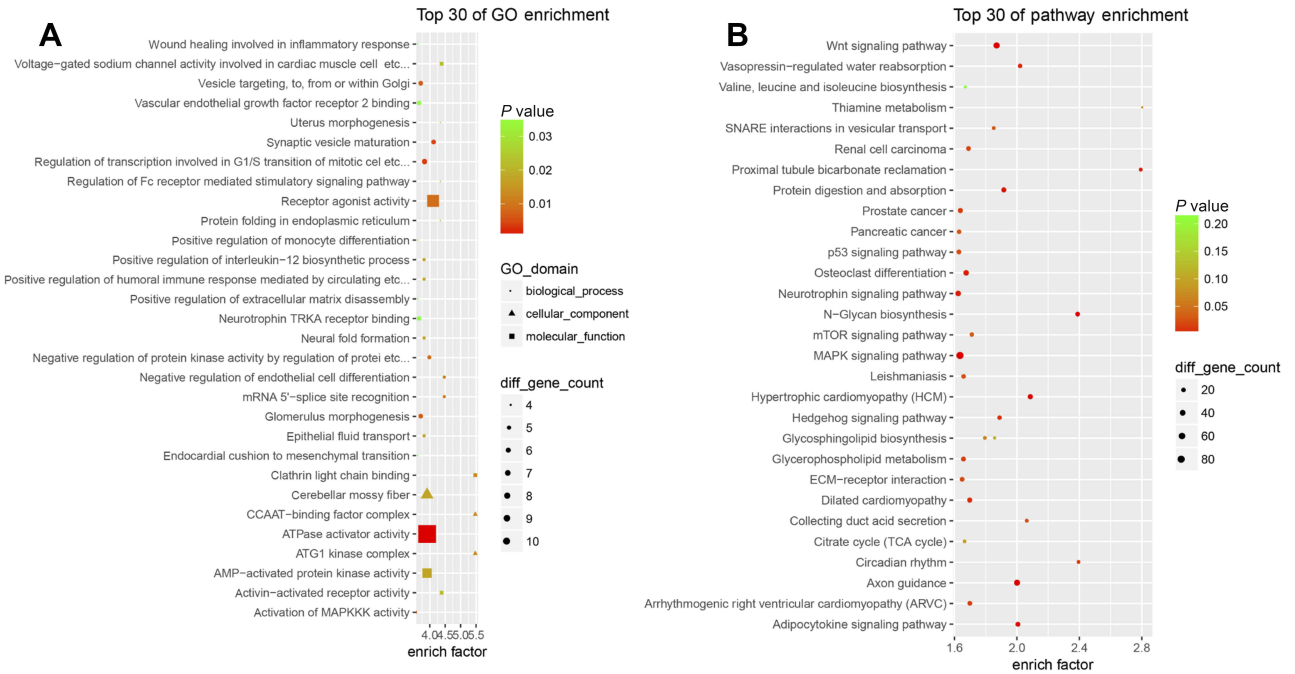

Figure 7 GO and KEGG analyses of potential target genes of circRNA-689. (**A**) Top 30 enrichment GOs. (**B**) T0 enrichment pathways.

kinase activity, and activation of MAPKKK activity. MF terms included MAPKKKK activity, VEGF receptor 2 binding, and others. The top 30 enrichment pathways that resulted from KEGG pathway analysis were VEGF signaling pathway, mTOR signaling pathway, ECM-receptor interaction, Wnt signaling pathway, and MAPK signaling pathway. These pathways are most likely involved in the progression of CGN.

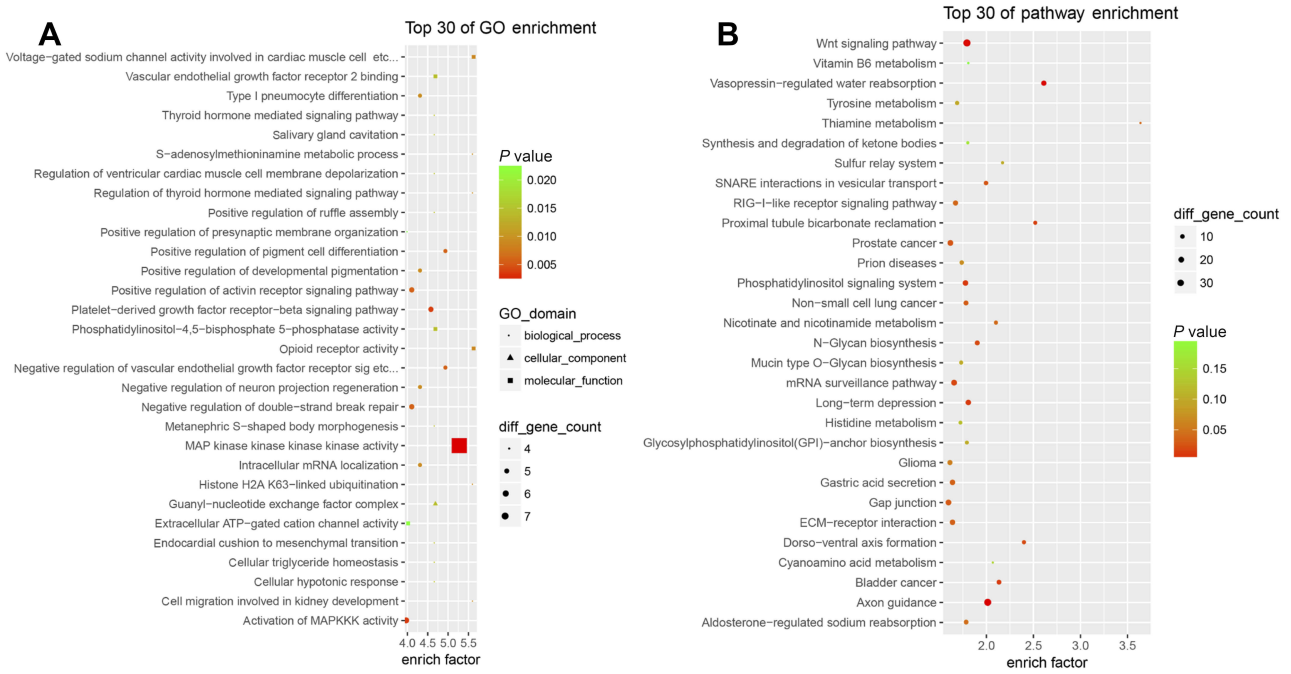

Figure 8 GO and KEGG analyses of potential target genes of circRNA-3217. (**A**) Top 30 enrichment GOs. (**B**) Top 30 enrichment pathways.

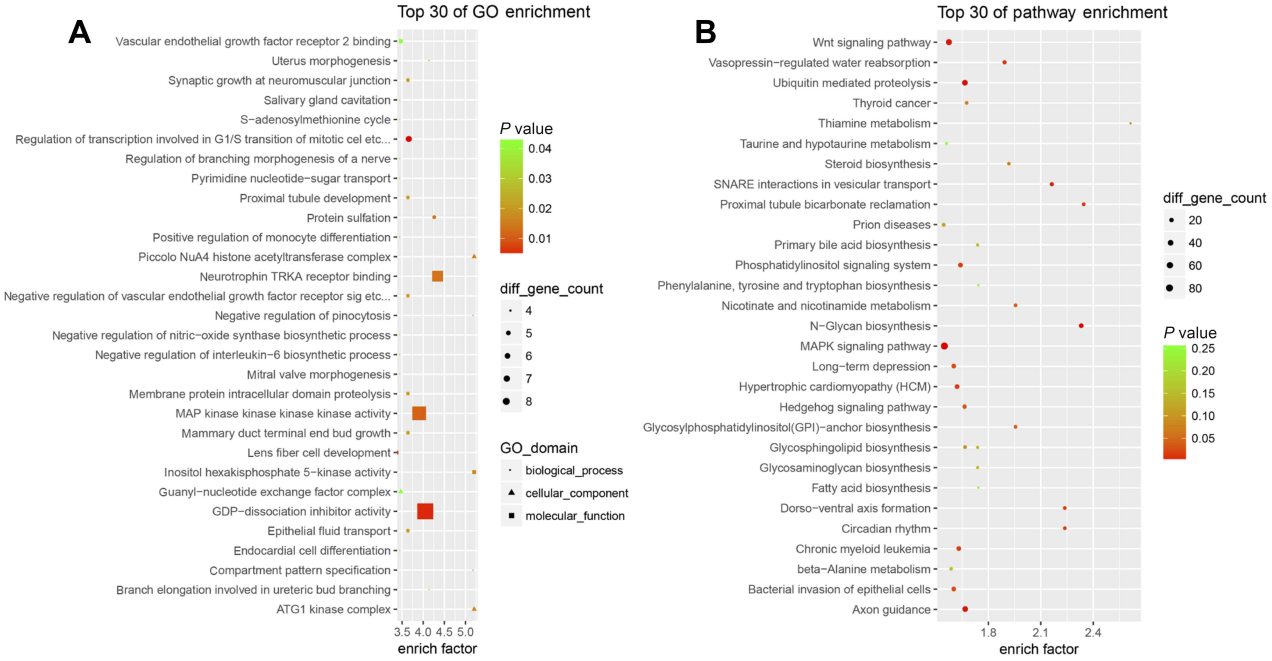

Figure 9 GO and KEGG analyses of potential target genes of circRNA-4907. (**A**) Top 30 enrichment GOs. (**B**) Top 30 enrichment pathways.

qRT-PCR validation

To verify the reliability of HTS data, four significantly DE circRNAs were validated by qRT-PCR. The related primers are listed in Table 3. The results agreed well with HTS data (Figure 10).

Discussion

Because TCM has multiple components, multiple targets, and multiple pathways, it is difficult to determine mechanisms. Development of transcriptome-sequencing (RNA-seq) has provided new methods for studying TCM. RNA-

Table 3 Primers used for qRT-PCR

Target ID	Primer sequences	PL (bp)
circRNA-213	F:5′CAAAGCTGAGGTGATGGCAG3′ R:5′TCAAGGATGGCAGTAACCCT3′	185
circRNA-689	F:5′TGGATCTGAAAAGTCTGCTGGA3′ R:5′GGTCCCAATGTTTGTGCTCTC3′	110
circRNA-3217	F:5′GATCAACACGGAGGATGAGGAA3′ R:5′AGCCATCCAAAACGGTGTC3′	92
circRNA-4907	F:5′TGCTTCTGTTGTCCTTACCCA3′ R:5′CTCCTCCTGCAAAGCCACT3′	163
GAPDH	F:5′TCCTGCACCACCAACTGCTTAG3′ R:5′AGTGGCAGTGATGGCATGGACT3′	102

Note: We used GAPDH as an internal control.
Abbreviations: F, forward; R, reverse; PL, product length.

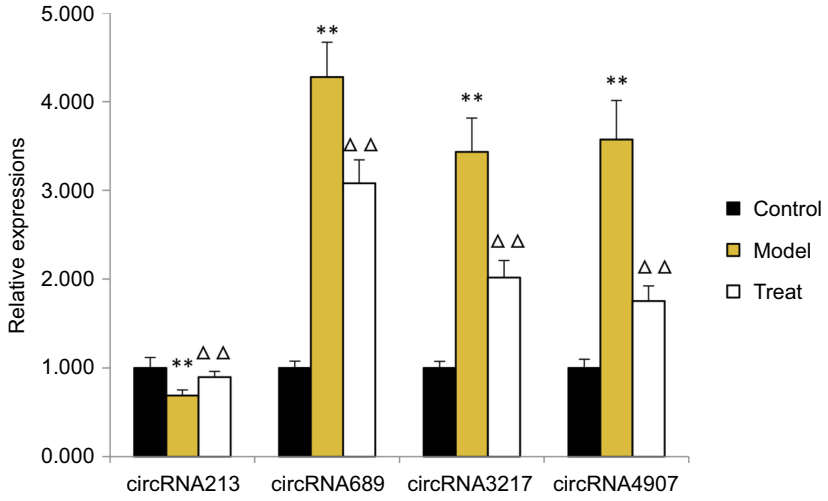

Figure 10 Validation of relative expression levels of circRNAs. GAPDH was used as an internal control. circRNA-213 was downregulated in the model group, and circRNA-689, circRNA-3217, and circRNA-4907 were upregulated. The qRT-PCR results are consistent with the HTS data.**P-value <0.01 between the model group and the control group. $^{\Delta\Delta}P$-value <0.01 between the model group and the QTXZG group.

seq technology is ideal for transcript analysis and has been heavily used in TCM research.[29,35]

Rats are ideal models for studying genetic correlates of kidney diseases. A previous study showed that the presence of circRNA in rat renal tissue and circRNA renal expression data from rat models could be applied for studying renal disease.[36] The adriamycin-induced CGN rat model is the animal model most similar to human CGN, and is widely used in the study of CGN.[3,37]

In this study, using next-generation RNA sequencing, we observed dysregulation of four circRNAs caused by the establishment of a CGN model. This dysregulation was reversed by treatment with QTXZG. CircRNAs are expressed in a tissue-specific manner and in pathological conditions, which suggests that circRNAs may play vital roles in human diseases.[38] Indeed, recent studies have demonstrated that circRNAs participated in many human diseases by sponging miRNAs.[25,26,39,40] In our study, many of the potential target miRNAs of the four reported circRNAs were related to kidney disease. A previous study indicated that miRNA-149-5p was related to cellular apoptosis proliferation and migration in renal cell carcinoma.[41] In addition, miR-346 could negatively regulate SMAD and improve renal function and glomerular pathology in a mouse model of diabetic nephropathy.[42] A previous study reported that miR-342-3p was significantly downregulated in cadmium-induced renal injury.[43] MiR-125b-5p played a vital role in kidney dysfunction and was closely associated with serum creatinine levels in obstructive renal injury.[44] Another study showed that

overexpression of miR-326-3p could alleviate renal fibrosis via the miR-326-3p/FcγRIII/TGF-β/Smad signaling pathway.[45] The interactions between miRNAs mentioned above and circRNAs are shown in Table 2.

Potential target mRNAs were used for GO function analysis and pathway analysis to annotate and estimate functions of these circRNAs. Notably, several significantly enriched pathways were reported to be closely linked to nephritis. The VEGF signaling pathway plays a vital role in the progression of renal fibrosis, which is the final common pathway of CGN.[46] Inflammation and fibrosis can be improved by inhibiting the mTOR signaling pathway.[47] KEGG analysis of DEGs between hypoxic and normal HK-2 cells revealed that upregulated genes were most enriched in ECM-receptor interaction, and hypoxia is vital in the development of CGN.[48] The Wnt signaling pathway is involved in CKD and renal fibrosis in patients and experimental animal models.[49] glomerular mesangial cells of rats, MAPK signaling pathways are critical for the synthesis of IL-6 and TNF-α, which are important in the inflammatory response.[50]

Conclusions

This study advanced our understanding of possible mechanisms of QTXZG in the treatment of CGN related to circRNAs, and identified novel circRNAs as potential critical therapeutic targets of CGN. Further study is needed to explore the exact functions of these four specific circRNAs in CGN.

Acknowledgments

This study was supported by the Nature Science Research Project of Anhui province (1808085MH276) and the Science and Technology Planning Project in Anhui province (1501ld04007).

Disclosure

The authors report no conflicts of interest in this work.

References

1. Amanuel A, Kalkidan H, Cristiana A, et al. Global, regional, and national under-5 mortality, adult mortality, age-specific mortality, and life expectancy, 1970-2016: a systematic analysis for the Global Burden of Disease Study 2016. *Lancet (London, England)*. 2017;390 (10100):1084–1150. doi:10.1016/S0140-6736(17)31833-0
2. Velciov S, Gluhovschi G, Timar R, et al. Urinary enzymatic markers (N-acetyl-beta-D-glucosaminidase) in assessing the tubulointerstitial compartment in chronic glomerulonephritis related to odontogenic foci. *Wien Klin Wochenschr*. 2016;128(3–4):102–108. doi:10.1007/s00508-015-0841-4
3. Gao JR, Qin XJ, Jiang H, Wang T, Song JM, Xu SZ. The effects of Qi Teng Xiao Zhuo granules, traditional Chinese medicine, on the expression of genes in chronic glomerulonephritis rats. *J Ethnopharmacol*. 2016;193:140–149. doi:10.1016/j.jep.2016.08.011
4. Qiu H, Fan W, Fu P, et al. General acteoside of Rehmanniae leaves in the treatment of primary chronic glomerulonephritis: a randomized controlled trial. *Afr J Tradit Complement Altern Med*. 2013;10 (4):109–115.
5. Cybulsky AV, Walsh M, Knoll G, et al. Canadian Society of Nephrology Commentary on the 2012 KDIGO clinical practice guideline for glomerulonephritis: management of glomerulonephritis in adults. *Am J Kidney Dis*. 2014;63(3):363–377. doi:10.1053/j.ajkd.2013.12.001
6. Kou J, Wu J, Yang HT, et al. Efficacy and safety of Shenyankangfu tablets for primary glomerulonephritis: study protocol for a randomized controlled trial. *Trials*. 2014;15:479. doi:10.1186/1745-6215-15-479
7. Lv F, Wang YP, Wang D. Experience of syndrome differentiation and treatment on CGN by Cao En-ze. *J Anhui TCM Coll*. 2010;29 (03):30–32.
8. Lv F, Zhang J. Study on the inheritance and development of Xin'an medicine from diagnosis and treatment of CGN experience by Cao En-ze. *Cjgmcm*. 2010;25(11):1974–1975.
9. Wang JF. Experience of Cao En-ze in the treatment of chronic nephritis. *J Chin Med Clin*. 2017;29(08):1236–1238.
10. Gu GG. *Sheng Nong Ben Cao Jing*. Peking: People's Medical Press; 1955:8.
11. Li SZ. *Ben Cao Gang Mu Essentials*. Guangzhou: Guangdong Science and Technology Press. 1988;267.
12. Zhang ZJ. *Jin Kui Yao Lue*. Vol. 15. Peking: TCM Ancient Books Press. 1997;15,24.
13. Liu JS, Fang Q, Hu SJ, et al. Clinical study of shenkang granule in the treatment of chronic glomerulonephritis. *Liaoning j tradit Chin Med*. 2007;34(02):171–172.
14. Mao YP, Wang YP, Cao EZ, et al. Shenkang infusion treat latent nephritis of deficient spleen and kidney. *J Zhejiang Univ Chin Med*. 2010;34(03):335–336.
15. Cao EZ, Dai XH, Fang Q, et al. Clinical reseach of Shenkang Granule in the treatment of chronic glomerulonephritis. *Anhui clin J Tradit Chin Med*. 1999;11(02):73–75.
16. Hu SJ, Cao EZ, Wang YP, et al. Clinical study on the therapeutic effect of shenkang granule on chronic glomerulonephritis. *J Chin Med Clin*. 2008;20(02):140–141.
17. Ren KJ, Wang YP, Hu SJ, et al. Effects of Shen Kang Granule on serum high sensitivity C- reactive protein and coagulation function in patients with chronic glomerulonephritis and spleen kidney deficiency syndrome. *J Anhui TCM Coll*. 2017;36 (04):16–19.
18. Wei LB, Gao JR, Shan L, et al. Effect of Qi Teng Xiao Zhuo Granule on the treatment and pathological morphology of adriamycin chronic glomerulonephritis in rats. *Pharmacol Clin Chin Med*. 2016;32 (01):149–151.
19. Gao JR, Wu X, Song JM, et al. Regulation of Qi Teng Xiao Zhuo Granule on Syk/Ras/c-Fos signaling pathway in rats with chronic glomerulonephritis. *Pharmacol Clin Chin Med*. 2017;33 (05):143–149.
20. Gao JR, Zhou CD. Orthogonal experiment on extraction process of Shenkang granule. *J Anhui TCM Coll*. 2004;23(05):44–46.
21. Wei LB, Wu X, Wang XY, et al. Study on quality control of Shenkang granule. *Chin J Inf TCM*. 2010;17(09):50–51.
22. Ge DD, Gao JR, Wu X, et al. Study on improvement of quality standard of Qi Teng Xiao Zhuo Granule. *Clin J Tradit Chin Med*. 2017;29(05):650–655.
23. Holdt LM, Kohlmaier A, Teupser D. Molecular roles and function of circular RNAs in eukaryotic cells. *Cell Mol Life Sci*. 2017;75:1071–1098.

24. Jeck WR, Sorrentino JA, Wang K, et al. Circular RNAs are abundant, conserved, and associated with ALU repeats. *RNA (New York, NY)*. 2013;19(2):141–157. doi:10.1261/rna.035667.112
25. Ma HB, Yao YN, Yu JJ, Chen XX, Li HF. Extensive profiling of circular RNAs and the potential regulatory role of circRNA-000284 in cell proliferation and invasion of cervical cancer via sponging miR-506. *Am J Transl Res*. 2018;10(2):592–604.
26. Luan J, Jiao C, Kong W, et al. circHLA-C plays an important role in lupus nephritis by sponging miR-150. *Mol Ther Nucleic Acids*. 2018;10:245–253. doi:10.1016/j.omtn.2017.12.006
27. Wang K, Sun Y, Tao W, Fei X, Chang C. Androgen receptor (AR) promotes clear cell renal cell carcinoma (ccRCC) migration and invasion via altering the circHIAT1/miR-195-5p/29a-3p/29c-3p/CDC42 signals. *Cancer Lett*. 2017;394:1–12. doi:10.1016/j.canlet.2016.12.036
28. Yan L, Feng J, Cheng F, et al. Circular RNA expression profiles in placental villi from women with gestational diabetes mellitus. *Biochem Biophys Res Commun*. 2018;498(4):743–750. doi:10.1016/j.bbrc.2018.03.051
29. Lang BJ, Holton KM, Gong J, Calderwood SK. A workflow guide to RNA-seq analysis of chaperone function and beyond. *Methods Mol Biol (Clifton, NJ)*. 2018;1709:233–252.
30. Hallas JM, Chichvarkhin A, Gosliner TM. Aligning evidence: concerns regarding multiple sequence alignments in estimating the phylogeny of the Nudibranchia suborder Doridina. Royal Society Open Science. 2017;4(10):171095.
31. Gao Y, Wang J, Zhao F. CIRI: an efficient and unbiased algorithm for de novo circular RNA identification. *Genome Biol*. 2015;16(1):4. doi:10.1186/s13059-015-0667-4
32. Robinson MD, McCarthy DJ, Smyth GK. edgeR: a Bioconductor package for differential expression analysis of digital gene expression data. *Bioinformatics*. 2010;26(1):139–140. doi:10.1093/bioinformatics/btp616
33. Pasquinelli AE. MicroRNAs and their targets: recognition, regulation and an emerging reciprocal relationship. *Nat Rev Genet*. 2012;13(4):271–282. doi:10.1038/nrg3162
34. Shannon P, Markiel A, Ozier O, et al. Cytoscape: a software environment for integrated models of biomolecular interaction networks. *Genome Res*. 2003;13(11):2498–2504. doi:10.1101/gr.1239303
35. Qu Z, Cui J, Harata-Lee Y, et al. Identification of candidate anti-cancer molecular mechanisms of Compound Kushen Injection using functional genomics. *Oncotarget*. 2016;7(40):66003–66019. doi:10.18632/oncotarget.11788
36. Cheng X, Joe B. Circular RNAs in rat models of cardiovascular and renal diseases. *Physiol Genomics*. 2017;49(9):484–490. doi:10.1152/physiolgenomics.00064.2017
37. Gao JR, Qin XJ, Jiang H, Wang T, Song JM, Xu SZ. Screening and functional analysis of DE genes in chronic glomerulonephritis by whole genome microarray. *Gene*. 2016;589(1):72–80. doi:10.1016/j.gene.2016.05.031
38. Han B, Chao J, Yao H. Circular RNA and its mechanisms in disease: from the bench to the clinic. *Pharmacol Ther*. 2018. doi:10.1016/j.pharmthera.2018.01.010
39. Jost I, Shalamova LA, Gerresheim GK, Niepmann M, Bindereif A, Rossbach O. Functional sequestration of microRNA-122 from Hepatitis C Virus by circular RNA sponges. *RNA Biol*. 2018;1–8. doi:10.1080/15476286.2018.1435248
40. Yang L, Han B, Zhang Y, et al. Engagement of circular RNA HECW2 in the nonautophagic role of ATG5 implicated in the endothelial-mesenchymal transition. *Autophagy*. 2017;1–70. doi:10.1080/15548627.2017.1332566
41. Jin L, Li Y, Liu J, et al. Tumor suppressor miR-149-5p is associated with cellular migration, proliferation and apoptosis in renal cell carcinoma. *Mol Med Rep*. 2016;13(6):5386–5392. doi:10.3892/mmr.2016.5205
42. Zhang Y, Xiao HQ, Wang Y, Yang ZS, Dai LJ, Xu YC. Differential expression and therapeutic efficacy of microRNA-346 in diabetic nephropathy mice. *Exp Ther Med*. 2015;10(1):106–112. doi:10.3892/etm.2015.2468
43. Fay MJ, Alt LAC, Ryba D, et al. Cadmium nephrotoxicity is associated with altered MicroRNA expression in the rat renal cortex. *Toxics*. 2018;6(1):16. doi:10.3390/toxics6010016
44. Wang S, Wu L, Du L, Lu H, Chen B, Bai Y. Reduction in miRNA-125b-5p levels is associated with obstructive renal injury. *Biomedical Rep*. 2017;6(4):449–454. doi:10.3892/br.2017.875
45. Wang Y, Zhang R, Zhang J, Liu F. MicroRNA-326-3p ameliorates high glucose and ox-LDL-IC- induced fibrotic injury in renal mesangial cells by targeting FcgammaRIII. *Nephrology (Carlton, Vic)*. 2017;23:1031–1038.
46. VHasegawa S, Nakano T, Torisu K, et al. Vascular endothelial growth factor-C ameliorates renal interstitial fibrosis through lymphangiogenesis in mouse unilateral ureteral obstruction. *Lab Invest*. 2017;97(12):1439–1452. doi:10.1038/labinvest.2017.77
47. Wang B, Ding W, Zhang M, Li H, Gu Y. Rapamycin attenuates aldosterone-induced tubulointerstitial inflammation and fibrosis. *Cell Physiol Biochem*. 2015;35(1):116–125. doi:10.1159/000369680
48. Yu W, Li Y, Wang Z, et al. Transcriptomic changes in human renal proximal tubular cells revealed under hypoxic conditions by RNA sequencing. *Int J Mol Med*. 2016;38(3):894–902. doi:10.3892/ijmm.2016.2677
49. Wang Y, Zhou CJ, Liu Y. Wnt Signaling in Kidney Development and Disease. *Prog Mol Biol Transl Sci*. 2018;153:181–207. doi:10.1016/bs.pmbts.2017.11.019
50. Ji M, Lu Y, Zhao C, et al. C5a induces the synthesis of IL-6 and TNF-alpha in rat glomerular mesangial cells through MAPK signaling pathways. *PLoS One*. 2016;11(9):e0161867. doi:10.1371/journal.pone.0161867